Targeting sequences of UBXD8 and AAM-B reveal that the ER has a direct role in the emergence and regression of lipid droplets

John K. Zehmer*, René Bartz*,‡, Blaine Bisel, Pingsheng Liu, Joachim Seemann and Richard G. W. Anderson§

Department of Cell Biology, University of Texas Southwestern Medical Center, Dallas, TX 75390, USA

*These authors contributed equally to this work
‡Present Address: Merck and Co., RNA Therapeutics, 770 Sumneytown Pike, West Point, PA 19486, USA
§Author for correspondence (richard.anderson@utsouthwestern.edu)

Accepted 19 July 2009
Journal of Cell Science 122, 3694-3702 Published by The Company of Biologists 2009
doi:10.1242/jcs.054700

Summary

Lipid droplets are sites of neutral lipid storage thought to be actively involved in lipid homeostasis. A popular model proposes that droplets are formed in the endoplasmic reticulum (ER) by a process that begins with the deposition of neutral lipids between the membrane bilayer. As the droplet grows, it becomes surrounded by a monolayer of phospholipid derived from the outer half of the ER membrane, which contains integral membrane proteins anchored by hydrophobic regions. This model predicts that for an integral droplet protein inserted into the outer half of the ER membrane to reach the forming droplet, it must migrate in the plane of the membrane to sites of lipid accumulation. Here, we report the results of experiments that directly test this hypothesis. Using two integral droplet proteins that contain unique hydrophobic targeting sequences (AAM-B and UBXD8), we present evidence that both proteins migrate from their site of insertion in the ER to droplets that are forming in response to fatty acid supplementation. Migration to droplets occurs even when further protein synthesis is inhibited or dominant-negative Sar1 blocks transport to the Golgi complex. Surprisingly, when droplets are induced to disappear from the cell, both proteins return to the ER as the level of neutral lipid declines. These data suggest that integral droplet proteins form from and regress to the ER as part of a cyclic process that does not involve traffic through the secretory pathway.

Supplementary material available online at
http://jcs.biologists.org/cgi/content/full/122/20/3694/DC1

Key words: Lipid droplet, Adiposome, Biogenesis, Regression, Sar1, Endoplasmic reticulum, ER

Introduction

Lipid droplets (LDs) are compartments found in most cell types that store neutral lipids such as triacylglycerol and cholesteryl ester. Because of its droplet morphology, this compartment has long been considered to be an inert container devoid of metabolic activity. Recent proteomic studies, however, have found that LDs are enriched in a variety of proteins known to be involved in lipid metabolism, membrane traffic and the structural integrity of the mono-phospholipid container (Athenstaedt et al., 1999; Brasaemle et al., 2004; Fujimoto et al., 2004; Liu et al., 2004; Murphy, 2001). Moreover, detailed lipidomic studies attest to the complexity and specialization of the lipid composition of this compartment (Bartz et al., 2007a; Murphy, 2001; Tauchi-Sato et al., 2002). On the basis of this new information, most now agree that LDs are organelles specialized for the regulation of cellular lipid metabolism, and function as a lipid-processing center for the cell.

Even though the proteomics and lipidomics evidence is compelling, a case for organelle status depends upon a clear understanding of the origin of this compartment. So far, little is known about this process. There are several models to explain droplet biogenesis. The most popular model proposes that droplets form when a lens of neutral lipids accumulates between the phospholipid bilayer of the ER. As the lens grows, it buds into the cytosol and becomes surrounded by a phospholipid monolayer derived from the outer ER bilayer (Murphy, 2001). Eventually the droplet pinches off from the ER. A second model proposes that droplets form in contact with the ER, but are not actually released from the ER membrane (Robenek et al., 2006). Neither model explains how integral and peripheral resident proteins are targeted to the droplet or how neutral lipids accumulate in certain membrane bilayers and not others. A parsimonious view is that the ER, or a related membrane, contains machinery that is required to coordinate the assembly of the various components necessary to build a functioning droplet. The same machinery probably assembles lipoproteins in cells that secrete this class of proteins (Murphy, 2001). We have suggested the name adiposome to designate the core biogenic machinery that builds and maintains this organelle (Liu et al., 2004).

In contrast to droplet formation, virtually nothing is known about how droplets regress. Most, if not all, cells respond to an excess of free fatty acid or cholesterol by enlarging the number and size of droplets. In turn, droplets disappear under metabolic conditions that consume the stored lipid. Even within the seemingly quiescent droplet, neutral lipids such as cholesteryl esters continuously recycle in a futile pathway that consumes ATP (Brown et al., 1980; McGookey and Anderson, 1983). As the balance shifts towards consumption of lipids, the droplets get smaller and major proteins such as ADRP and perilipin are degraded in the cytosol by the proteasome machinery (Masuda et al., 2006; Xu et al., 2006; Xu et al., 2005). The fate of the integral droplet proteins, by contrast, and the phospholipid monolayer in which they reside is not known. One possibility is that these

elements cycle back to the ER and become part of a ready pool for later droplet formation.

Elucidation of the mechanism of biogenesis and regression of droplets would be greatly aided by the availability of integral membrane proteins that mark the phospholipid monolayer surrounding the droplet during various phases of its life cycle. A candidate marker protein is caveolin-1, which under certain conditions will accumulate in droplets (Ostermeyer et al., 2001). This protein, however, is better known as a caveolae marker and is therefore unsuitable for our purposes. We chose instead to use a newly identified class of droplet proteins containing hydrophobic sequences that are necessary and sufficient for targeting to droplets. AAM-B and UBXD8 are two proteins in this class that we originally identified in a proteomic screen (Liu et al., 2004). Previously we showed that the N-terminal hydrophobic sequence of AAM-B is necessary and sufficient to target a protein to droplets (Zehmer et al., 2008). In the current work we have used both AAM-B and UBXD8 to follow the biogenesis and regression of droplets. We show that these proteins behave as integral membrane proteins that are inserted into the ER, transferred from their site of insertion to droplets independently of COPII vesicles and return to the ER when droplets are induced to regress. These findings suggest that droplets directly form from and return to the ER as part of a cyclic process of neutral lipid expansion and retraction.

Results

AAM-B and UBXD8 are attracted to forming lipid droplets

Previously, we showed that AAM-B is selectively located on the periphery of LDs. When expressed at high levels, however, AAM-B is also found in the ER (Zehmer et al., 2008). One explanation for these observations is that AAM-B is inserted into the ER, moves laterally in the plane of the ER membrane and collects in forming droplets. This model assumes that droplets have a limited capacity for accumulating AAM-B, so that any excess made in the ER remains there. To test this model, we set up conditions to see whether AAM-B would transfer from the ER to droplets. Normal rat kidney (NRK) cells have very few LDs (Bartz et al., 2007b). When we transfected these cells with AAM-B-Myc (Fig. 1A) and grew them for 8 hours, immunofluorescence using anti-Myc IgG had an ER staining pattern that matched that observed with anti-PDI IgG. No

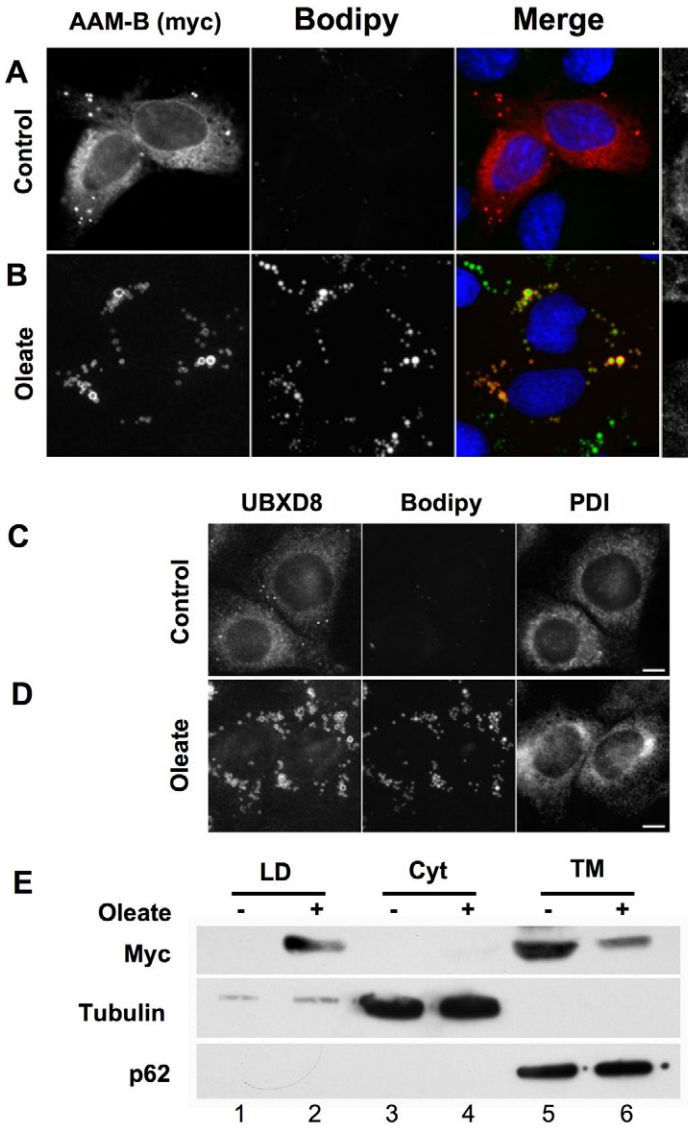

Fig. 1. AAM-B and UBXD8 traffic from ER to forming droplets. (A,B) NRK cells on coverslips were transfected with Myc-tagged AAM-B and grown for 8 hours. One set was fixed immediately (A) whereas the other was incubated further in the presence of 50 μg/ml cycloheximide plus oleic acid for 15 hours before fixation (B). The cells were processed for immunofluorescence detection of Myc (red). Neutral lipids were stained with Bodipy 493/503 (green) and DNA with Hoechst 33342 (blue). In uninduced cells, the majority of the staining has a reticular pattern indicative of ER (A). In oleic-acid-treated cells (B) the majority of staining surrounds Bodipy-493/503-positive droplets. Scale bar: 5 μm. (C,D) NRK cells cultured on coverslips were fixed (C) or grown in the presence of cycloheximide plus oleic acid for 15 hours (D). After fixation, cells were processed for immunofluorescence localization of UBXD8 and PDI. Neutral lipids were stained with Bodipy 493/503. In untreated cells, the majority of staining is present in a reticular pattern (C). Oleic acid treatment results in an induction of droplets. As for AAM-B, most of the UBXD8 now surrounds Bodipy-positive droplets (D). Scale bar: 5 μm. (E) CHO K2 cells stably expressing Myc-tagged AAM-B were pretreated with BFA for 8 hours to eliminate droplets. BFA was removed and the cells treated with cycloheximide and either oleic acid or ethanol for 15 hours. The cells were fractionated into droplets (LD), cytosol (Cyt) and total membranes (TM) and equal volumes separated by PAGE and immunoblotted with antibodies against the indicated protein or tag. In ethanol-incubated cells, AAM-B was found exclusively in membranes (lane 5). Incubation in the presence of oleic acid, by contrast, caused a substantial fraction of the AAM-B to move to the droplet fraction (lane 2), with a concomitant loss of AAM-B from the membrane fraction (lane 6). Tubulin and p62 were detected as cytosolic and ER controls, respectively.

lipid droplets were visible, as judged by staining with the fluorescent neutral lipid dye Bodipy. By contrast, when cells were grown under the same conditions followed by 15 hours in the presence of both 100 μM oleate and 50 μg/ml cycloheximide, the majority of the Myc IgG staining was on the surface of Bodipy-positive LDs (Fig. 1B). Identical results were obtained when we followed the fate of endogenous UBXD8 with anti-UBXD8 IgG (compare Fig. 1C with Fig. 1D).

We used cell fractionation to confirm these results in a different cell system (Fig. 1E). We established a Chinese hamster ovary K2 (CHO K2) cell line stably expressing C-terminal Myc-tagged AAM-B. Since CHO K2 cells have large numbers of droplets under standard culture conditions, we treated the cells for 8 hours with 2 μg/ml Brefeldin A (BFA) to deplete the droplet population (Bartz et al., 2007b). The drug was washed out and fresh medium added containing either 200 μM oleate plus 1 mg/ml BSA and ethanol or BSA and ethanol alone. Cycloheximide was again added to block protein synthesis before incubating in the presence of oleate. After 15 hours, the cells were fractionated into droplets, cytosol and total membranes and equal fractions were analyzed by immunoblotting (Fig. 1E). Under control conditions, AAM-B was found exclusively in the membrane fraction (Fig. 1E, lane 5). By contrast, oleate caused AAM-B to shift from the total membrane (Fig. 1E, compare lane 5 with 6) to the droplet fraction (Fig. 1E, compare lane 1 with 2).

These results suggest that in the absence of new protein synthesis AAM-B and UBXD8 that had been inserted into the ER moved directly to forming droplets. Three things need to be documented for this interpretation to be correct. First, we needed to determine whether protein synthesis was inhibited. We transfected cells with a cDNA encoding GFP with the C-terminus linked to the PEST domain of ornithine decarboxylase (residues 421-461), which forms an unstable protein with a half-life of ~2 hours (Li et al., 1998). The cells grew for 9 hours before adding either 50 μg/ml cycloheximide or ethanol carrier and grown for an additional 15 hours. Cells receiving the cycloheximide treatment did not contain any GFP whereas cells grown in the presence of ethanol had abundant GFP (supplementary material Fig. S1A). Second, we needed to show that AAM-B and UBXD8 are both integral membrane proteins (Fig. 2A). A post-nuclear supernatant was prepared from NRK cells transiently transfected with the cDNA encoding Myc-tagged AAM-B. This fraction was then washed with either buffer alone (Fig. 2A, lanes 1 and 2), 10 mM EDTA (Fig. 2A, lanes 2 and 3), 1 M KCl (Fig. 2A, lanes 5 and 6) or pH 11 Na carbonate (Fig. 2A, lanes 7 and 8). Membranes (M) were pelleted from the cytosol (S) by ultracentrifugation, separated by gel electrophoresis and immunoblotted with the indicated antibodies. The four-pass transmembrane protein Sec61α was found in the membrane fraction regardless of how samples were treated. The peripheral membrane protein GRASP55, which is anchored in the membrane by myristoylation and palmitylation, was shifted to the supernatant fraction by addition of sodium carbonate (pH 11), as expected. AAM-B remained in the membrane fraction under all conditions, which is the defining feature of an integral membrane protein. AAM-B also partitioned into the Triton X-114 detergent phase, along with Sec61α (Fig. 2B, lane 2). GRASP55 partitioned into the aqueous phase (Fig. 2B, lane 2). A similar result was obtained with UBXD8 (supplementary material Fig. S1B), although the putative membrane anchor for this protein is an interior hydrophobic sequence between residues 90 and 118. Finally, we needed to demonstrate that either AAM-B or UBXD8 could traffic from the ER to the droplet in the absence of lipid supplementation. We reasoned that if we attached a standard leader peptide to the N-terminus of AAM-B then the protein would be cleaved by the signal peptidase while AAM-B was being inserted into the ER (Fig. 2C). We used HeLa cells that had been grown in the absence of oleate. Cells were transfected with cDNAs encoding either wild-type AAM-B (WT), AAM-B with a hepatitis B virus precore protein signal sequence (HB), or the same signal sequence with the C-terminal

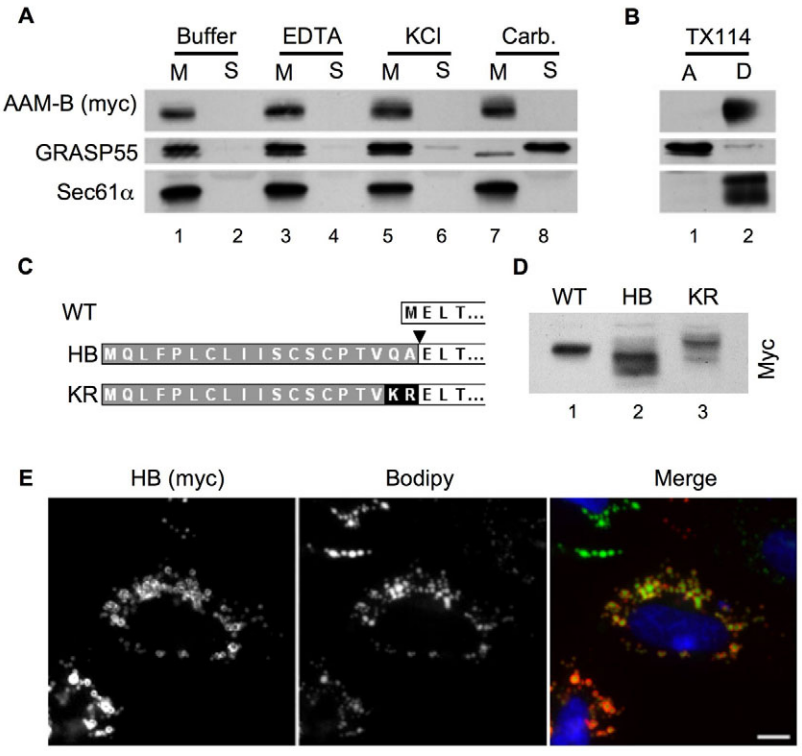

Fig. 2. AAM-B is an integral membrane protein made in the ER. Post nuclear supernatants (PNS) prepared from NRK cells transiently expressing Myc-tagged AAM-B were washed with either buffer alone, 10 mM EDTA, 1 M KCl or pH 11 sodium carbonate before centrifugation at 100,000 ***g***. The supernatants and pellets were separated by PAGE and analyzed by immunoblotting. (A) The peripheral membrane protein GRASP55 was extracted from the membranes by carbonate. By contrast, the transmembrane protein Sec61α and AAM-B were found in the membrane pellet under all conditions. (B) Triton-X114 partitioning of the PNS shows that GRASP55 is in the aqueous phase whereas Sec61α and AAM-B partitioned into the detergent phase. (C) Schematic representation of the N-terminal domain of wild-type AAM-B (WT) and two chimeras. The first chimera (HB) has the initiating methionine of AAM-B replaced with the signal sequence from Hepatitis B virus precore protein (highlighted in gray). The predicted signal peptidase cut site is labeled with an arrowhead. The second chimera (KR) is the same as the first but with the Q and A changed to K and R to eliminate the signal sequence cleavage site. (D) HeLa cells were transfected with cDNAs encoding the three constructs, lysates and processed for immunoblotting to detect the Myc tag. The HB construct (lane 2) migrated faster than the WT (lane 1) indicating that the signal sequence had been cleaved. By contrast, the KR construct migrates more slowly than the WT, indicating that the signal sequence has not been cleaved. (E) Cells from the experiment described in D were processed for immunofluorescence detection of Myc-tagged HB using anti-Myc IgG and neutral lipids with Bodipy 493/503. The HB chimera targeted to Bodipy-positive droplets. Scale bar: 5 μm.

amino acids Q and A changed to a K and R (KR) to block peptidase cleavage. Cells were grown for 15 hours before assaying for the expression of each construct (Fig. 2D) as well as the location of HB in the cell (Fig. 2E). The addition of an additional 18 amino acids on to wild-type AAM-B should cause it to migrate higher on the gel. Indeed anti-Myc IgG immunoblotting showed that the KR construct ran slower than the wild type (Fig. 2D, compare lane 3 with lane 1). By contrast the HB construct ran somewhat faster on the gel compared with WT (Fig. 2D, compare lane 2 with lane 1), suggesting that the leader peptide had been cleaved. We do not know why HB migrated faster than the WT, although the exact cleavage point for a signal peptidase is difficult to predict (Nielsen and Krogh, 1998). Nevertheless, this construct retained the ability to target endogenous droplets following insertion in the ER (Fig. 2E).

Typically, integral membrane proteins inserted in the rough ER either remain there or are transported to the Golgi complex in COPII-coated vesicles. A fundamental question is whether integral membrane droplet proteins such as AAM-B and UBXD8 bypass the canonical secretory pathway and travel directly to droplets or first exit the ER in COPII vesicles and migrate through the Golgi, before delivery to droplets in vesicles. Assembly of the COPII coats at the ER is dependent on the small GTPase Sar1. If AAM-B or UBXD8 is delivered to droplets via the secretory pathway, then blocking the action of Sar1 should prevent the two proteins from reaching droplets. We used microinjection to address this question (Fig. 3). We first determined whether a dominant-negative Sar1 (dnSar1p) (Aridor et al., 1995) had any effect on droplet formation (Fig. 3A,B). NRK cells were microinjected with dnSar1p along with an injection marker and cultured for 4 hours in the presence of either ethanol (Fig. 3A) or oleic acid dissolved in ethanol containing 1 mg/ml BSA (Fig. 3B) to induce droplet formation. The cells were then fixed and processed for detection of droplets (Bodipy), the Golgi-resident enzyme α-mannosidase II and an injection marker. Ethanol did not affect the organization of the Golgi complex (Fig. 3A, arrow, ethanol) and these cells did not have endogenous droplets. Since α-mannosidase II continuously cycles between the Golgi and the ER, it becomes trapped in the ER in cells injected with dnSar1p. Fig. 3A shows that α-mannosidase II had an ER distribution in dnSar1p-injected cells, whereas in non-injected cells, α-mannosidase II was localized to the Golgi (compare asterisk with arrow) (Altan-Bonnet et al., 2004). The presence of oleate in the medium caused droplet formation, even in cells injected with dominant-negative Sar1p (Fig. 3B, asterisk). Next, we looked at the ability of AAM-B and UBXD8 to reach droplets of dnSar1p-injected cells (Fig. 3C,D). In one trial, we co-injected dnSar1p with a cDNA encoding Myc-tagged AAM-B. In another experiment, we injected dnSar1p and followed the fate of endogenous UBXD8. The cells were injected, grown for 4 hours in the presence of oleic acid and then analyzed by immunofluorescence. dnSar1p caused α-mannosidase II to accumulate in the ER of injected cells (compare with Golgi of uninjected cells, Fig. 3C,D arrows), but both AAM-B and UBXD8 targeted correctly to droplets. We conclude that droplets form and acquire these integral membrane proteins directly from the ER without passing through CopII-coated vesicles.

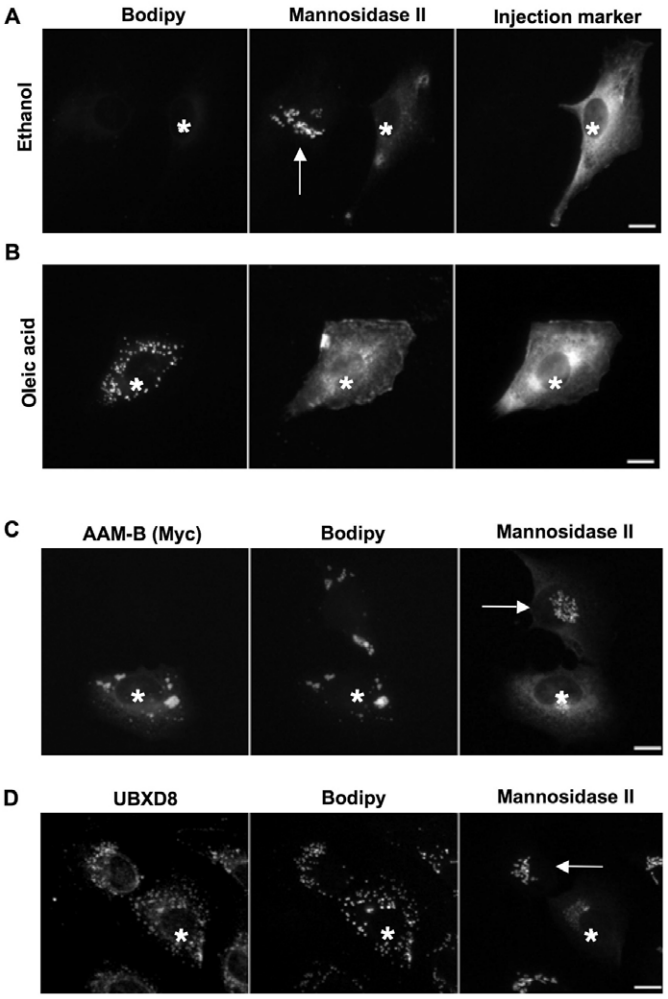

Fig. 3. Translocation of AAM-B and UBXD8 from the ER to LDs is independent of Sar1. (A) NRK cells were microinjected with recombinant, dominant-negative Sar1 to block ER exit and cultured for an additional 4 hours before processing for immunofluorescence (asterisk indicates injected cell). Since the Golgi-resident enzyme α-mannosidase II continuously cycles between the ER and Golgi, the block of ER exit in injected cells induces the relocation of α-mannosidase II from the Golgi to the ER. (B) Oleic acid supplementation leads to droplet formation despite the block of ER exit. (C) Cells were co-injected with the dominant-negative Sar1 and cDNA encoding AAM-B. AAM-B is made and trafficked to forming droplets despite the secretory blockade. (D) Endogenous UBXD8 reaches newly formed droplets despite injection of Sar1 dominant-negative protein. Asterisks indicate injected cells. Arrows point to Golgi of uninjected cells. Scale bars: 5 μm.

AAM-B and UBXD8 return to ER when droplets regress

Just as droplets form under conditions of fatty acid excess, they regress when cells are deprived of fatty acids. Little is known about the fate of droplet proteins when LDs disappear from the cell. Both ADRP (Masuda et al., 2006; Xu et al., 2005) and perilipin (Xu et al., 2006) are degraded by the ubiquitin-proteasome pathway when triacylglycerol recycling is disrupted by the long chain acyl-CoA synthetase inhibitor triacsin C. We used triacsin C to reduce LDs in the cell and followed the fate of transfected Myc-AAM-B. CHO K2 cells stably expressing Myc-tagged AAM-B were treated with cycloheximide, plus either triacsin C or DMSO as a vehicle control (Fig. 4). Cells were incubated for an additional 15 hours before droplets, cytosol and total membranes were purified by cell fractionation and processed for immunoblotting to detect ADRP, Myc, tubulin and Sec61α. In the absence of triacsin C, AAM-B was primarily in the LD fraction, along with ADRP (Fig. 4, lane 1). The presence of triacsin C shrunk the LD fraction, as indicated by the loss of ADRP (Fig. 4, lane 2). AAM-B also disappeared from the LD fraction but, unexpectedly, appeared in the total

membrane fraction (Fig. 4, lane 6). These results suggest that AAM-B is not degraded during droplet regression but instead moves to a membrane compartment. The level of tubulin in the cytosol (Fig. 4, lanes 3 and 4) and Sec61α in the total membrane (Fig. 4, lanes 5 and 6) did not change during the incubation.

We used immunofluorescence to identify the destination of AAM-B when droplets disappear from the cell. We transfected NRK cells with a cDNA encoding Myc-AAM-B and grew them for 3 hours before adding oleic acid to induce LDs (Fig. 5A,B). Cells were incubated an additional 6 hours and either fixed or incubated in the presence BSA, 7.5 μM triacsin C and cycloheximide for 15 hours before processing for immunofluorescence. AAM-B localized to LDs in cells with droplets (Fig. 5A). Cells treated with triacsin C, by contrast, lost all their droplets (Bodipy) and AAM-B was exclusively in PDI positive ER and nuclear envelope (Fig. 5B, AAM-B). The same result was obtained when endogenous UBXD8 was imaged (Fig. 5C,D). In the absence of protein synthesis, the AAM-B and UBXD8 in the ER could have only come from regressing LDs.

Discussion

ALDI (Turro et al., 2006), 17β-hydroxysteroid dehydrogenase type 11 (Yokoi et al., 2007), AAM-B, and UBXD8 appear to be integral membrane proteins inserted in the ER that can accumulate in LDs. The first three have a N-terminal ~28-residue hydrophobic sequence that anchors the protein in membranes and is necessary and sufficient [at least for AAM-B (Zehmer et al., 2008)] for targeting to LDs. UBXD8, by contrast, has an internal hydrophobic sequence between residues 90 and 118 that probably contains the LD-targeting information. The targeting information in the AAM-B hydrophobic sequence targets correctly when positioned internally in a GFP-AAM-B fusion protein (Zehmer et al., 2008). Other than being hydrophobic, the amino acid sequences of these targeting motifs are different. Nevertheless, there is something special about these sequences, because the N-terminal hydrophobic anchor of CYP2C9 cannot substitute for the N-terminal 28 amino acids of AAM-B. For convenience, we refer to proteins containing an integral LD targeting sequence as LDIMPs (lipid droplet integral membrane protein).

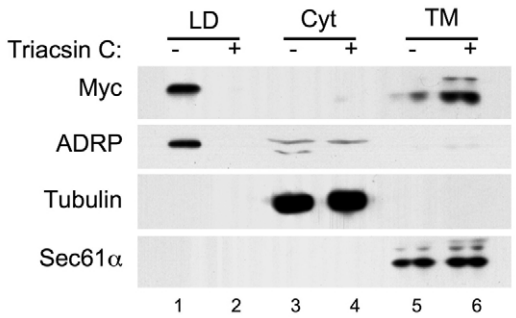

Fig. 4. AAM-B in droplets returns to a membrane fraction when droplets regress. CHOK2 cells stably expressing Myc-tagged AAM-B were treated with cycloheximide and either triacsin C or DMSO for 15 hours. The cells were fractionated into droplets (LD), cytosol (Cyt) and total membranes (TM) and equal volumes processed for immunoblotting to detect the indicated protein. In control cells, AAM-B-Myc was primarily in droplets (lane 1). Following incubation in the presence of triacsin C, the number of droplets declined as indicated by the loss of ADRP from the LD fraction (lane 2). By contrast, a large increase in the amount of AAM-B in the membrane fraction of the Triacsin C treated cells was observed (lane 6). The ER marker Sec61α remained in the total membrane fraction.

LDIMPs provide a new conceptual framework for understanding the biogenesis of LDs. These are integral membrane proteins that are inserted into the ER before moving to either endogenous (Fig. 2) or oleate-induced (Fig. 1) LDs without exiting the ER in COPII vesicles. In the absence of vesicle traffic, therefore, LDIMPs must reach droplets by moving laterally in the plane of the ER membrane. The hydrophobic targeting signal appears to be specialized for this process. This sequence probably does not span the ER membrane, yet is necessary and sufficient for correct targeting, even when placed in the middle of a protein (Zehmer et al., 2008). Therefore, it is an intrinsic property of these simple hydrophobic sequences to reside in the outer monolayer of the ER and move laterally in the plane of this monolayer before being sequestered by LDs. Unexpectedly, not only do LDIMPs collect in forming droplets induced by oleate, but also in LDs of cells not grown in the presence

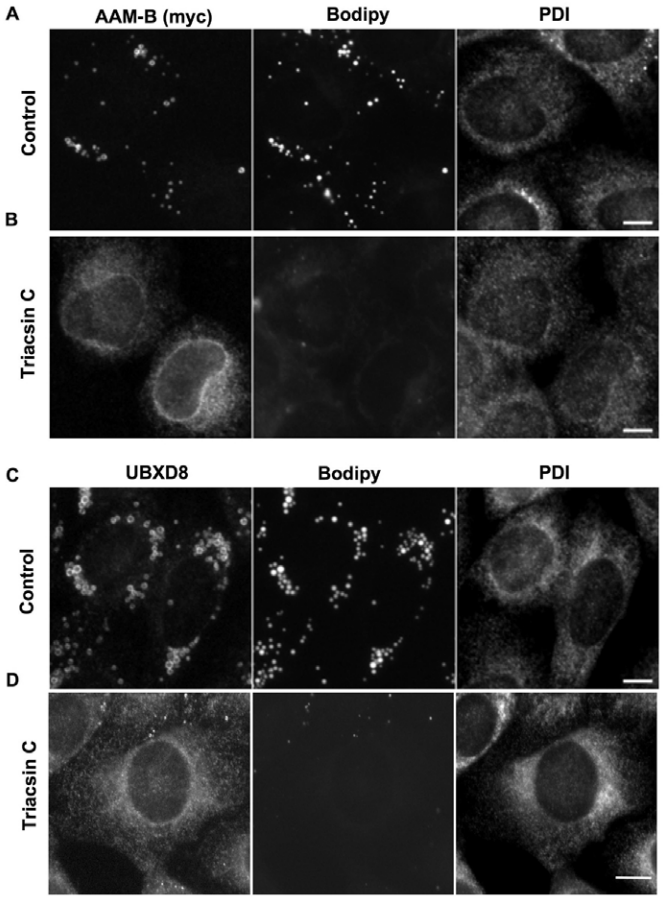

Fig. 5. AAM-B and UBXD8 on LDs return to the ER upon droplet regression. (A,B) NRK cells on coverslips were transfected with Myc-tagged AAM-B. Three hours after transfection, oleate was added and the cells incubated for an additional 6 hours. Cells were then either fixed (A) or incubated in the presence of 1 mg/ml BSA, 50 μg cycloheximide and 7.5 μg/ml triacsin C for 15 hours (B) before processing the samples for immunofluorescence. In the control cells the majority of AAM-B was detected surrounding Bodipy-positive droplets (A). In triacsin-C-treated cells, very few or no droplets were detected by Bodipy staining, and AAM-B was found in a reticular pattern (B). (C,D) NRK cells on coverslips were treated as in A and B, except they were not transfected and the endogenous UBXD8 was detected directly with anti-UBXD8 IgG. In the control cells, UBXD8 was found on Bodipy-positive droplets (C). By contrast, UBXD8 was found primarily in a reticular pattern that colocalized with PDI in the triacsin-C-treated cells (D). Scale bars: 5 μm.

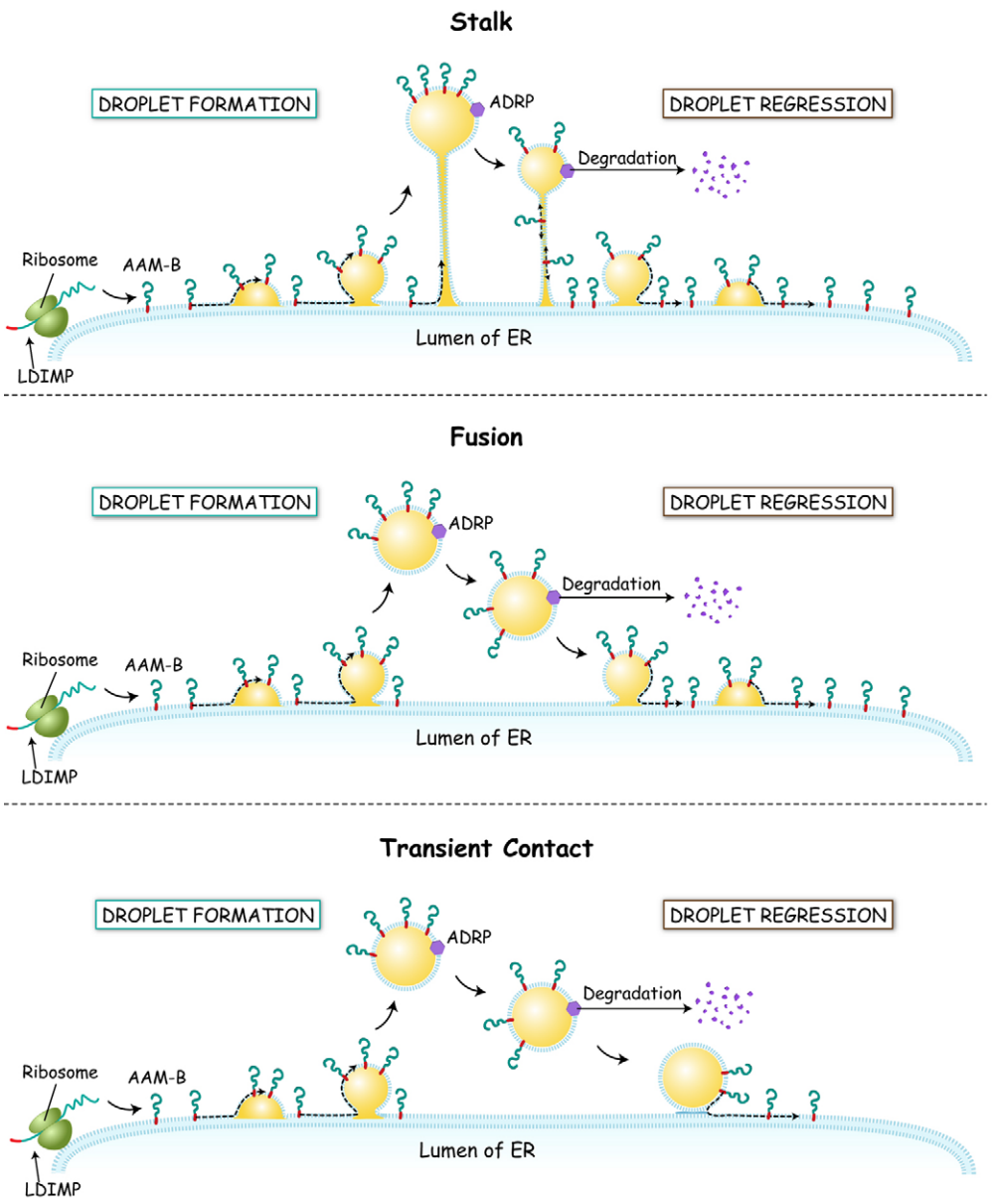

Fig. 6. Three models to explain how integral droplet proteins travel between ER and LD. (A) Stalk Model. LDIMP proteins such as AAM-B and UBXD8 move from the ER to droplets through a stalk composed of two phospholipid monolayers derived from the ER that remains continuous with LDs. During LD regression, LDIMPs migrate back to the ER through the stalk. (B) Fusion Model. LDIMPs move to form droplets that then bud from the ER to form free LDs. During droplet regression, the LD refuses with the ER and the LDIMPs return to the ER. (C) Transient Contact Model. LDIMPs move into droplets that bud from the ER. During droplet regression, the LD docks with the ER outer monolayer where it delivers the L-DIMP back to the ER without fusing.

oleate (Fig. 2C). In other words, the ability of LDIMPs to collect in LDs does not appear to be linked to incubation in the presence of oleate.

Because LDIMPs accumulate in LDs without passing through the Golgi complex when cells are grown in the presence of oleate, they serve as markers for sites of LD biogenesis. There is little doubt, therefore, that LDs are organelles generated by the ER. Another organelle that appears to arise directly from ER is the peroxisome. For many years, peroxisomes were considered to be semi-autonomous, self-replicating organelles, similar to mitochondria. This model is not consistent with the observation that several yeast mutants deficient in detectable peroxisomes can regain the organelle when transfected with a cDNA encoding a wild-type version of the mutant protein (Subramani, 1998). Recently, several groups observed the movement of integral membrane proteins from the ER to forming peroxisomes in yeast and mammalian cells (Hoepfner et al., 2005; Kim et al., 2006; Kragt et al., 2005; Tam et al., 2005). These observations have led to a new consensus that peroxisomes form from the ER (van der Zand et al., 2006). Similarly to the production of LDs, peroxisome biogenesis does not require integral membrane protein transport through the Golgi. For example, Pex2p, Pex3p and Pex16p are properly targeted to peroxisomes in the presence of inhibitors of COPII coat formation (Voorn-Brouwer et al., 2001). Similarly, the Golgi-disrupting drug Brefeldin A does not prevent PMP70 or Pex3p from targeting to peroxisomes (Toro et al., 2007). Brefeldin A and a dominant-negative Sar1 mutant also do not prevent AtPEX2 and AtPEX10 from reaching peroxisomes (Sparkes et al., 2005). It is likely that peroxisomes and LDs form from separate specialized regions of ER. Interestingly, yeast peroxisomes that are unable to oxidize fatty acids form tight, membrane-dependent associations with LDs. This suggests that peroxisomes and LDs can form extensive membrane-membrane contacts that are important for coordinating the lipolysis of LD triacylglycerol with oxidation of fatty acids in peroxisomes (Binns et al., 2006). In addition, many LDs are rich in monoalk(en)yl diacylglycerol that are synthesized in part by enzymes that reside

in peroxisomes (Bartz et al., 2007a). It might be more than a coincidence that two major organelles known to be involved in regulating lipid metabolism are made by the ER.

Although LDs appear to arise from special machinery in the ER, recent studies suggest that COP I (Beller et al., 2008; Soni et al., 2009) and COP II (Soni et al., 2009) coats can regulate the amount of neutral lipids stored in droplets. They appear to do so, in part, by delivering LD molecules such as ATGL and ADRP to droplets. Exactly how COP proteins mediate this delivery process is unclear, but might involve novel functions for a class of proteins traditionally viewed as membrane budding coats. Thus, LDs can acquire various molecules after they initially form in the ER.

The discovery that LDIMPs made in the ER can migrate to forming droplets apparently without passing through the Golgi is consistent with existing models for how LDs form during neutral lipid accumulation (Murphy, 2001). There is not a model, however, to explain how LDIMPs reach endogenous droplets that presumably existed at the time the cells were transfected with the cDNA. One possibility is that LDs never detach from the ER, therefore LDIMPs access droplets through a stalk of phospholipid monolayer (Fig. 6A); in the second, LDIMPs move from the ER into droplets that have either fused (Fig. 6B) or docked (Fig. 6C) transiently with the ER. Presently, we cannot distinguish between these two models, although each predicts that a tight interaction between LDs and ER is necessary for LD biogenesis and maintenance.

Several studies have documented that ADRP is degraded by the ubiquitin-proteasome pathway during droplet regression (Masuda et al., 2006; Xu et al., 2006). By contrast, we found that LDIMPs return to the ER where they appear largely to be preserved. This suggests that the phospholipid monolayer surrounding each LD returns to the ER when neutral lipid is depleted. The return of LDIMPs to the ER is essentially the reciprocal of LDIMP movement to existing droplets (Fig. 6). If LDs are always attached to the ER through a thin stalk (Fig. 6A) then LDIMPs can easily return through the stalk. The stalk, in other words, functions as a conduit through which droplet LDIMPs can travel to and from the ER. If, however, LDs do detach from the ER, then LDIMPs must return by monolayer fusion (Fig. 6B) or through transient contact sites (Fig. 6C). If LDIMPs return at transient contact sites then there would have to be a mechanism for disposing of the LD phospholipid monolayer. However, returning by LD fusion with the ER monolayer would require specialized membrane fusion machinery capable of selectively fusing phospholipid monolayers but not bilayers. Thus, the stalk model is the most parsimonious of the three and can account for both the fate of the monolayer, the return of LDIMPs to the ER and the movement of LDIMPs to existing droplets. This model is also consistent with the many transmission EM studies showing that ER tends to be associated with LDs (e.g. McGookey and Anderson, 1983). Unfortunately, transmission EM is not a good method for unequivocally identifying the stalks, because the tight apposition of the two monolayers in the stalk would appear as a simple membrane bilayer of unknown origin.

One of the attractive aspects of the LD stalk model is the possibility that phospholipid monolayer stalks function as interorganelle connectors that facilitate the movement of specialized integral membrane proteins and their cargo between different membrane-bound compartments. Presumably, proteins capable of traveling through these connectors would have different functions in each compartment. For example, we demonstrate that UBXD8, which belongs to a family of proteins that regulate ubiquitylation, is able to move between ER and LDs and that the steady state location of the protein depends on whether cells have LDs. UBXD8 is a newly identified component of the mammalian dislocation machinery, which is a multiprotein complex that is essential for moving damaged ER membrane proteins to the cytoplasm for degradation by the 20S proteasome (Lee et al., 2008; Mueller et al., 2008). Immunoprecipitation experiments suggest that UBXD8 interacts with valosin-containing protein (p97/VCP) (Lee et al., 2008). p97/VCP belongs to the AAA ATPase family of proteins and appears to have a crucial role in the extraction of these proteins from membranes for proteasome degradation. Our findings raise the possibility that UBXD8 controls the localization of p97/VCP. In cells rich in LDs, most of the UBXD8-p97 and associated proteins are in droplets, whereas in cells with few droplets, these proteins are in the ER. Indeed, proteomics shows that isolated droplets contain both UBXD8 and p97/VCP (Liu et al., 2004; Bartz et al., 2007c). Rapid changes in the size of the lipid store might have a dramatic affect on the location of these proteins and, therefore, the function of the proteasome degradation pathway. Whether UBXD8-p97 is active in droplets and/or the ER remains to be determined.

Materials and Methods

Antibodies and reagents

The anti-GRASP55 pAb was raised in rabbits against the C-terminal domain of rat GRASP55 fused to GST. The anti-p62 pAb was a kind gift from Dorothy Mundy (U.T. Southwestern Medical Center, Dallas, TX). The anti-Myc clone 4A6 mAb and anti-Sec61α pAb were from Upstate Biotechnology (Charlottesville, VA). The anti-PDI pAb was from Stressgen (Ann Arbor, MI). Anti-α-mannosidase II was from Kelly Moremen (The University of Georgia, Athens, GA). We purchased anti-ADRP from Fitzgerald Industries International (Concord, MA). Goat anti-UBXD8 was from Novus Biologicals (Littleton, CO). Alexa Fluor 488-, 568- and 647-conjugated secondary antibodies, cascade-blue conjugated bovine serum albumin (BSA), Hoechst 33342, Lipofectamine 2000 and Bodipy 493/503 were from Invitrogen (Carlsbad, CA). The HRP-conjugated secondary antibodies and Bradford dye were from Bio-Rad (Hercules, CA). Protease inhibitor cocktail III was obtained from Calbiochem (San Diego, CA). The enhanced chemiluminescent substrate (ECL) was from Pierce (Milwaukee, WI). Triacsin C was from Biomol (Plymouth Meeting, PA). Brefeldin A was from Epicenter Technologies (Madison, WI). DMEM and BSA were from Sigma (St Louis, MO). The recombinant dominant-negative Sar1 protein (dnSar1p) was made and purified as described (Rowe and Balch, 1995). Cosmic calf serum and fetal bovine serum were from HyClone (Logan, UT). G418 was from Research Products International (Mt Prospect, IL).

Cell culture

Normal rat kidney (NRK) and CHO K2 cells were grown in DMEM (4.5 g/l glucose), 10% Cosmic calf serum and 40 μg/ml proline. HeLa cells were grown in the same medium, but with 10% fetal bovine serum. The CHO K2 stable line was generated using standard protocols and single clones were maintained with 300 μg/ml G418.

cDNA constructs

Preparation of the AAM-B cDNA was described (Zehmer et al., 2008). The destabilized GFP construct was made using primer overlap extension PCR to join nucleotides coding for residues 421-461 of mouse ornithine decarboxylase, which contains a PEST sequence, to the 3′ end of GFP. This construct was ligated into pcDNA3.1. The constructs were confirmed by sequencing.

Modification of AAM-B signal sequence

HeLa cells grown in 6 cm dishes containing coverslips were transfected using Fugene 6 (Roche) with cDNA encoding wild-type AAM-B, HepB-AAM-B or mutant HepB-AAM-B and grown overnight. The coverslips were removed and processed for immunofluorescence localization of AAM-B. The remaining cells were scraped into PAGE sample buffer, sonicated, boiled for 5 minutes, separated by PAGE and analyzed by immunoblotting.

EDTA, salt and carbonate washing and Triton X-114 partitioning

NRK cells were grown in a 15 cm dish to 90% confluence and then transfected with 32 μg cDNA encoding AAM-B using Lipofectamine 2000 according to the manufacturer's protocol. The cells were further incubated in standard media for 15 hours. Nontransfected cells were used for the UBXD8 experiment. The cells were scraped into PBS containing 200 μM PMSF, pelleted and resuspended in buffer A (250 mM sucrose, 20 mM Tris-HCl, pH 7.4) containing a protease inhibitor cocktail. The cells were incubated on ice for 20 minutes and then broken by five passes through a 22 G needle. The lysates were centrifuged at 1000 ***g*** for 7 minutes to generate the

post-nuclear supernatant (PNS). For the washing experiments, aliquots of the PNS were mixed 1:1 with the following buffers: TBS (140 mM NaCl, 20 mM Tris-HCl, pH 7.4), EDTA (20 mM EDTA, 20 mM Tris-HCl, pH 7.4), salt (2 M KCl, 20 mM Tris-HCl, pH 7.4) or carbonate (200 mM sodium carbonate, pH 11) for a final volume of 500 µl. The samples were incubated on ice for 1 hour and were then layered on 300 µl cushion buffer 1 (500 mM sucrose, 20 mM Tris-HCl, pH 7.4) in a microcentrifuge tube and centrifuged for 30 minutes at 100,000 ***g*** in a TLA55 rotor. The supernatants and pellets were recovered and proteins were precipitated with trichloroacetic acid (TCA). The cushion was discarded. The TCA pellets were washed with acetone, resuspended in 2× SDS sample buffer, boiled for 5 minutes, separated by PAGE and analyzed by immunoblotting. For the Triton X-114 partitioning experiments (Bordier, 1981), an aliquot of PNS was mixed 1:1 with extraction buffer (150 mM NaCl, 1% Triton X-114, 10 mM Tris-HCl, pH 7.4) for a final volume of 200 µl. The sample was incubated for 10 minutes on ice and then 3 minutes at 37°C and then layered on 300 µl cushion buffer 2 (150 mM NaCl, 0.06% Triton X-114, 6% sucrose, 10 mM Tris-HCl, pH 7.4). The sample was then centrifuged at 200 ***g*** for 2 minutes. The supernatant was then re-extracted with extraction buffer and layered on the same cushion and treated as before. The supernatant and pellet were recovered and precipitated by the addition of acetone. The cushion was discarded. The samples were resuspended in 2× sample buffer, boiled for 5 minutes, separated by PAGE and analyzed by immunoblotting. These experiments were conducted twice.

Immunofluorescence

For immunofluorescence, coverslips were washed twice with PBS and then fixed in 4% formaldehyde in PBS for 20 minutes at room temperature. The cells were permeabilized with 0.1% Triton X-100 in PBS for 5 minutes. The coverslips were incubated sequentially for 20 minutes at 37°C in primary antibody, followed by fluorescent conjugated secondary antibodies, both diluted in 1 mg/ml BSA in PBS. In some cases neutral lipids were stained with Bodipy 493/503 diluted 1:100 from a 1 mg/ml stock in DMSO. DNA was stained with Hoechst 33342 dye. The cells were viewed using a Zeiss (Oberkochen, Germany) AxioPlan 2E fluorescence microscope using a ×63 Apochromat, 1.40 NA lens and fitted with a Hamamatsu ORCA 100 (Hamamatsu City, Japan) monochromatic digital camera. Images were captured using OpenLab software from Improvision (Lexington, MA) and pseudocolored using Adobe Photoshop (San Jose, CA).

Droplet induction experiments

For the biochemical experiments, a CHO K2 cell line stably expressing Myc-tagged AAM-B was grown to ~90% confluence in four 15 cm dishes. The cells were treated for 8 hours with 2 µg/ml Brefeldin A to regress droplets. The medium was then replaced with complete medium containing 1 mg/ml BSA, 50 µg/ml cycloheximide and either 200 µM oleic acid (from 100 mM stock in ethanol) or ethanol as a vehicle control. The cells were cultured for an additional 15 hours. The cells were then scraped into PBS containing 200 µM PMSF, collected by centrifugation, resuspended in 800 µl buffer A and incubated on ice for 20 minutes. The cells were broken by five passes through a 22 G needle. A PNS was prepared by centrifugation at 1000 ***g*** for 7 minutes. The PNS was layered on top of 300 µl of cushion buffer 1 and centrifuged for 30 minutes at 100,000 ***g*** in a TLA55 rotor. The supernatant (excluding the cushion) was transferred to a fresh tube and the droplets were floated to the top by centrifugation at 10,000 ***g*** for 4 minutes. The underlying cytosol was recovered to a fresh tube using a gel-loading tip until droplets drawn from the top reached the bottom of the tube. This process was repeated until 100 µl of fluid remained. The remaining sample was overlaid with 300 µl buffer B (100 mM KCl, 2 mM $MgCl_2$, 20 mM HEPES, pH 7.4) and centrifuged for a final time. Then, 150 µl of the underlying fluid was removed and discarded leaving partially purified droplets. The cushion from the 100,000 ***g*** centrifugation was discarded and the total membrane pellet was washed with buffer A and then resuspended in 100 µl buffer A. The protein concentrations of the membrane and cytosol were determined by Bradford assay. All samples were precipitated by addition of 100% acetone followed by centrifugation at 20,800 ***g*** for 10 minutes. The pellets were resuspended in sample buffer and boiled for 5 minutes. Equal cellular fractions of the droplets, total membrane and cytosol were separated by PAGE and then analyzed by immunoblotting.

For immunofluorescence analysis NRK cells were grown to ~60% confluence on glass coverslips. The cells were transfected with cDNA using Lipofectamine 2000 according to the manufacturer's protocol and then incubated for an additional 8 hours. Untransfected cells were used for the UBXD8 experiments. One set of coverslips was fixed and stored in PBS at 4°C. The remaining cells were treated with 1 mg/ml BSA, 50 µg/ml cycloheximide and 100 µM oleic acid for an additional 15 hours. The remaining cells were then fixed and coverslips were processed for immunofluorescence. For the destabilized GFP experiments, cells were transfected and treated as above, except duplicate conditions were included that lacked cycloheximide. The biochemistry and microscopy experiments were conducted three times with representative results shown.

Droplet regression experiments

These experiments were conducted using methods similar to the droplet induction experiments with the following modifications. For biochemical analysis CHO K2 cells or a CHO K2 cell line stably expressing Myc-tagged AAM-B was grown in four 15-cm dishes. The cells were treated with medium containing 50 µg/ml cycloheximide and either 7.5 µM triacsin C or DMSO as a vehicle control and cultured an additional 15 hours. The cells were then fractionated and analyzed in a manner identical to the droplet induction experiments.

For the microscopy experiments, NRK cells were grown to ~60% confluence on glass coverslips. The cells were transfected with cDNA using Lipofectamine 2000 according to the manufacturer's protocol and then incubated for an additional 3 hours. Untransfected cells were used for the UBXD8 experiments. The medium was then replaced with complete medium containing 1 mg/ml BSA and 100 µM oleic acid and cultured for 6 hours. One set of coverslips was fixed and stored in PBS at 4°C. The medium on the remaining cells was replaced with complete medium containing 1 mg/ml BSA, 50 µg/ml cycloheximide and 7.5 µM triacsin C and the cells were incubated for s further 15 hours. The remaining cells were fixed and all coverslips were processed for immunofluorescence. The biochemistry and microscopy experiments were conducted three times with representative results shown.

Sar1 dominant negative microinjection

NRK cells were grown on coverslips and then microinjected with a dominant-negative recombinant Sar1 (1 mg/ml) along with 5 mg/ml cascade-blue-conjugated BSA as described (Bartz et al., 2008). At least 30 cells were injected per experiment. The cells were then cultured for 4 hours in the presence of 100 µM oleic acid or ethanol as a vehicle control. In other experiments dominant-negative Sar1 (1 mg/ml) and cDNA encoding Myc-tagged AAM-B (0.1 mg/ml) were co-injected into the nuclei of NRK cells. After incubation for 4 hours in the presence of 100 µM oleic acid, the cells were fixed and processed for immunofluorescence. Each experiment was conducted at least twice.

We thank Charles Hall for his valuable technical assistance and Brenda Pallares for her administrative assistance. This work was supported by grants from the National Institutes of Health, HL 20948, GM 52016, GM 70117, the Perot Family Foundation and the Cecil H. Green Distinguished Chair in Cellular and Molecular Biology. Deposited in PMC for release after 12 months.

References

Altan-Bonnet, N., Sougrat, R. and Lippincott-Schwartz, J. (2004). Molecular basis for Golgi maintenance and biogenesis. *Curr. Opin. Cell Biol.* **16**, 364-372.

Aridor, M., Bannykh, S. I., Rowe, T. and Balch, W. E. (1995). Sequential coupling between copii and copi vesicle coats in endoplasmic reticulum to Golgi transport. *J. Cell Biol.* **131**, 875-893.

Athenstaedt, K., Zweytick, D., Jandrositz, A., Kohlwein, S. D. and Daum, G. (1999). Identification and characterization of major lipid particle proteins of the yeast saccharomyces cerevisiae. *J. Bacteriol.* **181**, 6441-6448.

Bartz, R., Li, W. H., Venables, B., Zehmer, J. K., Roth, M. R., Welti, R., Anderson, R. G., Liu, P. and Chapman, K. D. (2007a). Lipidomics reveals that adiposomes store ether lipids and mediate phospholipid traffic. *J. Lipid Res.* **48**, 837-847.

Bartz, R., Seemann, J., Zehmer, J. K., Serrero, G., Chapman, K. D., Anderson, R. G. and Liu, P. (2007b). Evidence that mono-Adp-ribosylation of Ctbp1/bars regulates lipid storage. *Mol. Biol. Cell* **18**, 3015-3025.

Bartz, R., Zehmer, J. K., Zhu, M., Chen, Y., Serrero, G., Zhao, Y. and Liu, P. (2007c). Dynamic activity of lipid droplets: protein phosphorylation and Gtp-mediated protein translocation. *J. Proteome Res.* **6**, 3256-3265.

Bartz, R., Sun, L. P., Bisel, B., Wei, J. H. and Seemann, J. (2008). Spatial separation of Golgi and Er during mitosis protects Srebp from unregulated activation. *EMBO J.* **27**, 948-955.

Beller, M., Sztalryd, C., Southall, N., Bell, M., Jackle, H., Auld, D. S. and Oliver, B. (2008). Copi complex is a regulator of lipid homeostasis. *PLoS Biol.* **6**, e292.

Binns, D., Januszewski, T., Chen, Y., Hill, J., Markin, V. S., Zhao, Y., Gilpin, C., Chapman, K. D., Anderson, R. G. and Goodman, J. M. (2006). An intimate collaboration between peroxisomes and lipid bodies. *J. Cell Biol.* **173**, 719-731.

Bordier, C. (1981). Phase separation of integral membrane proteins in triton X-114 solution. *J. Biol. Chem.* **256**, 1604-1607.

Brasaemle, D. L., Dolios, G., Shapiro, L. and Wang, R. (2004). Proteomic analysis of proteins associated with lipid droplets of basal and lipolytically stimulated 3t3-L1 adipocytes. *J. Biol. Chem.* **279**, 46835-46842.

Brown, M. S., Ho, Y. K. and Goldstein, J. L. (1980). The cholesteryl ester cycle in macrophage foam cells: continual hydrolysis and re-esterification of cytoplasmic cholesteryl esters. *J. Biol. Chem.* **255**, 9344-9352.

Fujimoto, Y., Itabe, H., Sakai, J., Makita, M., Noda, J., Mori, M., Higashi, Y., Kojima, S. and Takano, T. (2004). Identification of major proteins in the lipid droplet-enriched fraction isolated from the human hepatocyte cell line Huh7. *Biochim. Biophys. Acta* **1644**, 47-59.

Hoepfner, D., Schildknegt, D., Braakman, I., Philippsen, P. and Tabak, H. F. (2005). Contribution of the endoplasmic reticulum to peroxisome formation. *Cell* **122**, 85-95.

Kim, P. K., Mullen, R. T., Schumann, U. and Lippincott-Schwartz, J. (2006). The origin and maintenance of mammalian peroxisomes involves a de novo Pex16-dependent pathway from the Er. *J. Cell Biol.* **173**, 521-532.

Kragt, A., Voorn-Brouwer, T., van den Berg, M. and Distel, B. (2005). Endoplasmic reticulum-directed Pex3P routes to peroxisomes and restores peroxisome formation in a saccharomyces cerevisiae Pex3Delta strain. *J. Biol. Chem.* **280**, 34350-34357.

Lee, J. N., Zhang, X., Feramisco, J. D., Gong, Y. and Ye, J. (2008). Unsaturated fatty acids inhibit proteasomal degradation of Insig-1 at a postubiquitination step. *J. Biol. Chem.* **283**, 33772-33783.

Li, X., Zhao, X., Fang, Y., Jiang, X., Duong, T., Fan, C., Huang, C. C. and Kain, S. R. (1998). Generation of destabilized green fluorescent protein as a transcription reporter. *J. Biol. Chem.* **273**, 34970-34975.

Liu, P., Ying, Y., Zhao, Y., Mundy, D. I., Zhu, M. and Anderson, R. G. (2004). Chinese hamster ovary K2 cell lipid droplets appear to be metabolic organelles involved in membrane traffic. *J. Biol. Chem.* **279**, 3787-3792.

Masuda, Y., Itabe, H., Odaki, M., Hama, K., Fujimoto, Y., Mori, M., Sasabe, N., Aoki, J., Arai, H. and Takano, T. (2006). Adrp/adipophilin is degraded through the proteasome-dependent pathway during regression of lipid-storing cells. *J. Lipid Res.* **47**, 87-98.

McGookey, D. J. and Anderson, R. G. (1983). Morphological characterization of the cholesteryl ester cycle in cultured mouse macrophage foam cells. *J. Cell Biol.* **97**, 1156-1168.

Mueller, B., Klemm, E. J., Spooner, E., Claessen, J. H. and Ploegh, H. L. (2008). Sel1L nucleates a protein complex required for dislocation of misfolded glycoproteins. *Proc. Natl. Acad. Sci. USA* **105**, 12325-12330.

Murphy, D. J. (2001). The biogenesis and functions of lipid bodies in animals, plants and microorganisms. *Prog. Lipid Res.* **40**, 325-438.

Nielsen, H. and Krogh, A. (1998). Prediction of signal peptides and signal anchors by a hidden markov model. *Proc. Int. Conf. Intell. Syst. Mol. Biol.* **6**, 122-130.

Ostermeyer, A. G., Paci, J. M., Zeng, Y., Lublin, D. M., Munro, S. and Brown, D. A. (2001). Accumulation of caveolin in the endoplasmic reticulum redirects the protein to lipid storage droplets. *J. Cell Biol.* **152**, 1071-1078.

Robenek, H., Hofnagel, O., Buers, I., Robenek, M. J., Troyer, D. and Severs, N. J. (2006). Adipophilin-enriched domains in the Er membrane are sites of lipid droplet biogenesis. *J. Cell Sci.* **119**, 4215-4224.

Rowe, T. and Balch, W. E. (1995). Expression and purification of mammalian sarl. *Methods Enzymol.* **257**, 49-53.

Soni, K. G., Mardones, G. A., Sougrat, R., Smirnova, E., Jackson, C. L. and Bonifacino, J. S. (2009). Coatomer-dependent protein delivery to lipid droplets. *J. Cell Sci.* **122**, 1834-1841.

Sparkes, I. A., Hawes, C. and Baker, A. (2005). Atpex2 and Atpex10 are targeted to peroxisomes independently of known endoplasmic reticulum trafficking routes. *Plant Physiol.* **139**, 690-700.

Subramani, S. (1998). Components involved in peroxisome import, biogenesis, proliferation, turnover, and movement. *Physiol. Rev.* **78**, 171-188.

Tam, Y. Y., Fagarasanu, A., Fagarasanu, M. and Rachubinski, R. A. (2005). Pex3P initiates the formation of a preperoxisomal compartment from a subdomain of the endoplasmic reticulum in Saccharomyces cerevisiae. *J. Biol. Chem.* **280**, 34933-34939.

Tauchi-Sato, K., Ozeki, S., Houjou, T., Taguchi, R. and Fujimoto, T. (2002). The surface of lipid droplets is a phospholipid monolayer with a unique fatty acid composition. *J. Biol. Chem.* **277**, 44507-44512.

Toro, A., Arredondo, C., Cordova, G., Araya, C., Palacios, J. L., Venegas, A., Morita, M., Imanaka, T. and Santos, M. J. (2007). Evaluation of the role of the endoplasmic reticulum-Golgi transit in the biogenesis of peroxisomal membrane proteins in wild type and peroxisome biogenesis mutant cho cells. *Biol. Res.* **40**, 231-249.

Turro, S., Ingelmo-Torres, M., Estanyol, J. M., Tebar, F., Fernandez, M. A., Albor, C. V., Gaus, K., Grewal, T., Enrich, C. and Pol, A. (2006). Identification and characterization of associated with lipid droplet Protein **1**, a novel membrane-associated protein that resides on hepatic lipid droplets. *Traffic* **7**, 1254-1269.

van der Zand, A., Braakman, I., Geuze, H. J. and Tabak, H. F. (2006). The return of the peroxisome. *J. Cell Sci.* **119**, 989-994.

Voorn-Brouwer, T., Kragt, A., Tabak, H. F. and Distel, B. (2001). Peroxisomal membrane proteins are properly targeted to peroxisomes in the absence of copi- and copii-mediated vesicular transport. *J. Cell Sci.* **114**, 2199-2204.

Xu, G., Sztalryd, C., Lu, X., Tansey, J. T., Gan, J., Dorward, H., Kimmel, A. R. and Londos, C. (2005). Post-translational regulation of Adrp by the ubiquitin/proteosome pathway. *J. Biol. Chem.* **280**, 42841-42847.

Xu, G., Sztalryd, C. and Londos, C. (2006). Degradation of perilipin is mediated through ubiquitination-proteasome pathway. *Biochim. Biophys. Acta* **1761**, 83-90.

Yokoi, Y., Horiguchi, Y., Araki, M. and Motojima, K. (2007). Regulated expression By Pparalpha and unique localization of 17beta-hydroxysteroid dehydrogenase Type 11 protein in mouse intestine and liver. *FEBS J.* **274**, 4837-4847.

Zehmer, J. K., Bartz, R., Liu, P. and Anderson, R. G. (2008). Identification of a novel N-terminal hydrophobic sequence that targets proteins to lipid droplets. *J. Cell Sci.* **121**, 1852-1860.